Real-Time QCM-D Monitoring of Cellular Responses to Different Cytomorphic Agents

Resubmitted to:

Biosensors & Bioelectronics

December 15th, 2010

JULIEN FATISSON[*,1], FERESHTEH AZARI[2] and NATHALIE TUFENKJI[1]

[1]Department of Chemical Engineering, McGill University,
Montreal, Quebec H3A 2B2, Canada
[2]Department of Molecular Physiology and Biophysics, University of Vermont,
Burlington, Vermont 05403, USA

[*] Corresponding Author. Phone: (514) 661-0730; Fax: (514) 398-6678; E-mail: julien.fatisson@gmail.com

Abstract

Quartz crystal microbalance with dissipation monitoring (QCM-D) is used for real-time *in situ* detection of cytoskeletal changes in live primary endothelial cells in response to different cytomorphic agents; namely, the surfactant Triton-X 100 (TX-100) and bacterial lipopolysaccharide (LPS). Reproducible dissipation versus frequency (*Df*) plots provide unique signatures of the interactions between endothelial cells and cytomorphic agents. While the QCM-D response for TX-100 can be described in two steps (changes in the osmotic pressure of the medium prior to observing the expected cell lysis), LPS results in a different single-phase signal. A complementary analysis is carried out to evaluate the possible competitive effects of TX-100 and LPS through the QCM-D response to BAEC stress by analyzing the *Df* plots obtained. Experiments with non-toxic components (fibronectin or serum) produce another different QCM-D response than that observed for the toxic chemicals, suggesting the use of *Df* plot signatures for the possible differentiation between cytotoxic or non-cytotoxic effects. Observations obtained by QCM-D signals are confirmed by conducting fluorescence microscopy at the same time. Our results show that a fast (few minutes) sensing response can be obtained *in situ* and in real-time. The conclusions from this study suggest that QCM-D can potentially be used in biodetection for applications in drug screening tests and diagnosis.

Keywords: *Bovine Aortic Endothelial Cells; Lipopolysaccharide; Triton-X 100; Quartz Crystal Microbalance; Dissipation factor; Fluorescence Microscopy*

1. Introduction

Cells possess numerous intrinsic properties such as growth, repair, degradation self-diagnosis, and protein and gene expression. They respond in very specific ways to different types of perturbations, allowing them to be used as biointerfaces for the detection of molecules interfering with a cell's activity. Cells respond to stressful agents by complex pathways that often lead to cytoskeletal changes to the cells, that can be detected using different techniques, such as microscopy or flow cytometry (Basu et al. 1999; Hosoya et al. 1993; Kabir-Salmani et al. 2002; Rotsch and Radmacher 2000; Walter et al. 1998; Yamaguchi et al. 1993). Although these measurement techniques are generally sensitive and useful, their implementation requires that the cells be lysed or fixed, hence rendering these techniques unsuitable for real-time *in situ* characterization of cell health.

Acoustic biosensors are now widely recognized and used to investigate eukaryotic cells in real-time and *in situ* (Cooper and Singleton 2007). Among the various acoustic transducers available, the quartz crystal microbalance (QCM) is commonly used to monitor changes in mass at the quartz crystal sensing surface (Sauerbrey 1959). QCM has been used to monitor the attachment kinetics of osteoblasts (Redepenning et al. 1993) or endothelial cells (Zhou et al. 2000) to solid surfaces and these studies suggested that this technique could be extended to monitor cells' responses to stressful environments. Marx et al. developed a sensitive QCM biosensor with living bovine aortic endothelial cells (BAEC) to detect microtubule alterations (Marx et al. 2001) and other dynamic cellular changes upon reaction with cytoskeleton binding drugs (Marx et al. 2007). More recently, Alessandini et al. (2006) confirmed by QCM the increase in cell rigidity of fibroblasts incubated with colchicines, which increase polymerization of the actin cytoskeleton.

Pioneering works using the QCM showed that viscoelastic properties of films deposited on the sensor surface can be examined using frequency changes (Kanazawa and Gordon 1985; Okahata et al. 1989). However, measurement of *f* alone is not easily and specifically related to structural or conformational changes occurring at the sensor surface, especially for cytoskeletal changes that imply cellular volume and mass redistribution over the adhesion surface. Additionally, the energy dissipation needs to be monitored to detect cytoskeletal changes because cell responses can be interpreted (or modeled) as a purely liquid effect as well as a purely elastic mass effect (Marx et al. 2003). Most real scenarios are actually in between these two limits. Rodahl et al. (1996; 1997) extended the QCM technique by performing the direct monitoring of energy dissipation (*D*) considered a useful indicator of the viscoelastic properties of the material deposited at the sensor surface. Among the different QCM-D investigations of cells, it was showed that the interaction between cells and a surface produced a unique and reproducible dissipation against frequency (*Df*) plot, also considered as a QCM-D signature (Fredriksson et al. 1998a; 1998b; Lord et al. 2006).

The results of the aforementioned studies raise interesting questions regarding the early stages of cell response, the influence of drug/chemical concentration, and the characteristics of the chemical perturbation on the cell morphology, thus motivating the need for further research into detection limits and response kinetics of QCM based whole-cell biosensors. Others have correlated the QCM signals and morphological changes with microscopy techniques but this has been done with cells that were extracted from their nutritive environment (i.e., fixed) (Elsom et al. 2008; Lord et al. 2009; Marx et al. 2001; Modin et al. 2006; Redepenning et al. 1993). Simultaneous microscopy observations and QCM-D signal detection would therefore act as a direct confirmation of frequency and energy dissipation changes. The aim of the present study is

to extend the applicability of the QCM-D technique and show that rapid, unique, and reproducible responses can be obtained.

In this study, we show that the early stages (first few minutes) of cytoskeletal changes can be detected and result in a reproducible and characteristic QCM-D signal. Two cytomorphic agents (Triton-X 100 and bacterial lipopolysaccharide) were used to induce specific cell responses. Triton-X 100 (TX-100) is one of the most common non-ionic detergents used for intracellular labeling by permeabilizing cell membranes via the solubilization of membrane proteins (Potgieter et al. 2009). Secondly, bacterial lipopolysaccharides (LPS) cause changes in the actin cytoskeleton and transendothelial permeability resulting in endothelial cell injury in bovine aortic cells (Chakravortty et al. 2000; Goldblum et al. 1993; Meyrick et al. 1989; 1986). Combinations of TX-100 and LPS were used to evaluate if these chemicals and their effects on cells would act in competition with regards to the QCM-D response. QCM-D was also used to examine the biosensor signature in the presence of fibronectin, a non-cytotoxic agent. The response of the QCM-D biosensor was confirmed by direct observation using fluorescence microscopy while frequency and dissipation signals were being recorded.

2. Materials and methods

2.1. Cytomorphic agents

Lyophilized LPS O55:B5 and Triton-X 100, obtained from Sigma-Aldrich, were dissolved in phosphate buffer saline solution (PBS) (Sigma-Aldrich) at a stock concentration of 5 mg/mL, and 10% (100 mg/mL), respectively. Human Fibronectin (HFN) was purchased from Sigma-Aldrich. Further dilution from these stock solutions into cell culture medium was carried out to the desired concentrations. All chemicals were analytical grade reagents, unless otherwise noted.

2.2. Cell culture

Bovine Aortic Endothelial Cells (BAEC), derived from the aorta of cattle inspected by the United States Department of Agriculture, were obtained from Cell Applications Inc. (CA, USA). BAEC culture was maintained in a humidified incubator (5% CO_2, 37°C) and was cultured on a gelatin-coated cell culture flask with F12-K medium, supplemented with 10% heat inactivated horse serum (HS), 100 U/mL of penicillin (Invitrogen), 100 µg/mL streptomycin (Invitrogen) and 30 µg/mL endothelial mitogen (Biomedical Technologies Inc, MA, USA). When the cell cultures reached 80-90% confluence, they were trypsinized (using 0.25% Trypsin in EDTA solution, Invitrogen), centrifuged at 3000 RPM for 3 minutes and resuspended in fresh medium. Cells were subsequently diluted 5-10 fold for the next passage. BAEC were seeded at 5×10^4 cells/mL on poly-L-lysine modified QCM-D crystals or glass slides and incubated at 37°C and 5% CO_2 for 24 h prior to any measurement.

2.3. Quartz Crystal Microbalance with Dissipation monitoring

QCM-D measurements were performed with a Q-Sense E4 unit (Q-Sense AB, Göteborg, Sweden) by simultaneously monitoring the shifts in frequency (Δf) and energy dissipation (ΔD) of a 5 MHz silica-coated QCM-D crystal (QSX-303) at different overtones. Detailed QCM-D principle and experimental procedures are provided in Supplementary Information. Briefly, a suspension of 5×10^4 BAEC was incubated on each Poly-L-Lysine (PLL)-modified quartz crystal for 24 hours (37°C, 5% CO_2), prior to being mounted into a clean flow chamber (QFM401, Q-Sense). Warmed fresh culture medium (37°C) was injected to reach a stable baseline, before injecting warmed culture medium (37°C) supplemented with the chemical of interest for at least

10 min. At least 3 independent experiments (different BAEC cultures) were carried out for each condition in order to calculate the averages and standard deviations presented in Table S1. Because the *D* factor is a ratio of energies (eq 1 in SI), it is dimensionless and is reported as 10^{-6} dissipation units (DU).

2.4. Microscopic observations

2.4.1. Fluorescence microscopy

Simultaneous fluorescence imaging and QCM-D measurements were performed for selected conditions using a window module (QWM401, Q-Sense). In contrast to the basic flow chamber, the window module has a glass window at the top that allows direct *in situ* observation of the crystal sensor with a fluorescence microscope (Olympus BX51). After the 24 h incubation used for cell attachment (as described above), BAEC covering the quartz crystals were gently rinsed with PBS once, then incubated in a solution of 50 µg/mL of Alexa Fluor 488 wheat germ agglutinin in PBS for 20 minutes (5% CO_2, 37°C) for fluorescent labeling, then gently rinsed twice with fresh pre-warmed medium. After cell labeling, the modified quartz crystal sensors were mounted into the flow chamber in order to perform *f* and *D* measurements along with fluorescence microscopy observations. Fluorescing BAEC were observed using the appropriate filter (EX between 460 nm and 490 nm, EM between 510 nm and 550 nm) with a CCD camera.

2.4.2 Scanning Electron Microscopy

A suspension of 5×10^4 cells/mL was seeded on PLL-coated glass coverslips (1 cm diameter) for 24 hours at 37°C and 5% CO_2. Supernatant was then removed and replaced with fresh medium for at least 30 minutes prior to cell exposure to the different chemical stressors for another 30

minutes. After rinsing with warmed non-supplemented culture medium, the BAEC were then fixed with 2.5% glutaraldehyde in PBS overnight. Surfaces were then dehydrated using ethanol/water solutions (increasing the ethanol proportion from 30% to 100%) and amyl acetate/ethanol solutions, (increasing the amyl acetate proportion from 25% to 100%). Surfaces were gold-palladium coated prior to observations using field emission gun scanning electron microscopy (FEG-SEM, Hitachi S-4700).

2.5. Statistical significance

An ANOVA (SAS) was employed to determine whether or not a statistically significant difference was observed between experiments. Results with $p < 0.05$ were considered statistically significant.

3. Results and discussion

3.1. Real-time QCM-D response during exposure to Triton-X 100

Triton-X 100 (TX-100) is a non-ionic surfactant commonly used in the manufacture of several influenza vaccines, such as Fluzone from Sanofi-Pasteur, and as a detergent in biochemistry investigations (Ives et al. 1986; Tufenkji et al. 2010). It acts as a membrane disrupter having an effect on the cytoskeleton and leading to cell lysis (Potgieter et al. 2009). TX-100 will induce important cytoskeletal changes that can be investigated in the QCM-D model through changes in Δf and ΔD signals. Because TX-100 micelles may possibly affect the cells in a different way than their monomeric equivalents, all experiments were conducted above the critical micelle concentration (0.01% (Rosenthal and Koussaie 1983)) in order to avoid such concerns. Figures

1a,b respectively show the frequency and dissipation signals obtained for different concentrations of TX-100 solutions incubated with adhered BAEC. Sharp decreases in both Δf and ΔD are observed when TX-100 is interacting with BAEC. A greater response is noted with increasing concentrations of TX-100. The first part of Δf and ΔD changes with time is referred to as Phase I and appears clearly on the *Df* plot (Figure 1c). A decrease in Δf suggests that more mass is detected at the crystal surface (Sauerbrey 1959). Since the *D* factor increases with material viscoelasticity, low *D* factors suggest that the material is generally rigid. Since both Δf and ΔD decrease in Phase I, the results measured during Phase I (Figure 1c) indicate that more rigid mass is detected at the surface. This phase is very short at 0.1% TX-100 (i.e., 1.5 minutes), while it lasted for the entire timescale of experiments for lower TX-100 concentrations. No statistically significant difference (p=0.94) was observed between the values of *Df* slopes measured for each TX-100 concentration (Table S1). Phase II is only observable for 0.1% TX-100 and is characterized by a frequency increase while ΔD continues to slowly drop. A Δf increase implies a mass removal from the sensor surface and therefore Phase II could be attributable to cell lysis induced by TX-100 at high concentrations (Potgieter et al. 2009).

Figure 1. Representative QCM-D measurements (a) frequency and (b) dissipation shifts, (1st overtone) for BAEC response to different concentrations of TX-100 as a function of time and (c), *Df* plot resulting from (a) and (b) curves: 0.1 % TX-100 (■ symbols and solid line), 0.05% TX-100 (□ symbols and dashed line) and 0.01% TX-100 (× symbols and dotted line). Phase I: hyperosmotic medium effect, and Phase II: cell lysis is occurring. (d), (e) and (f), schematic diagrams representing (d) a non-treated resting cell compared to the likely theory for the effects of TX-100: (e) hyperosmotic effect, Phase I, and (f) cell lytic effect, Phase II.

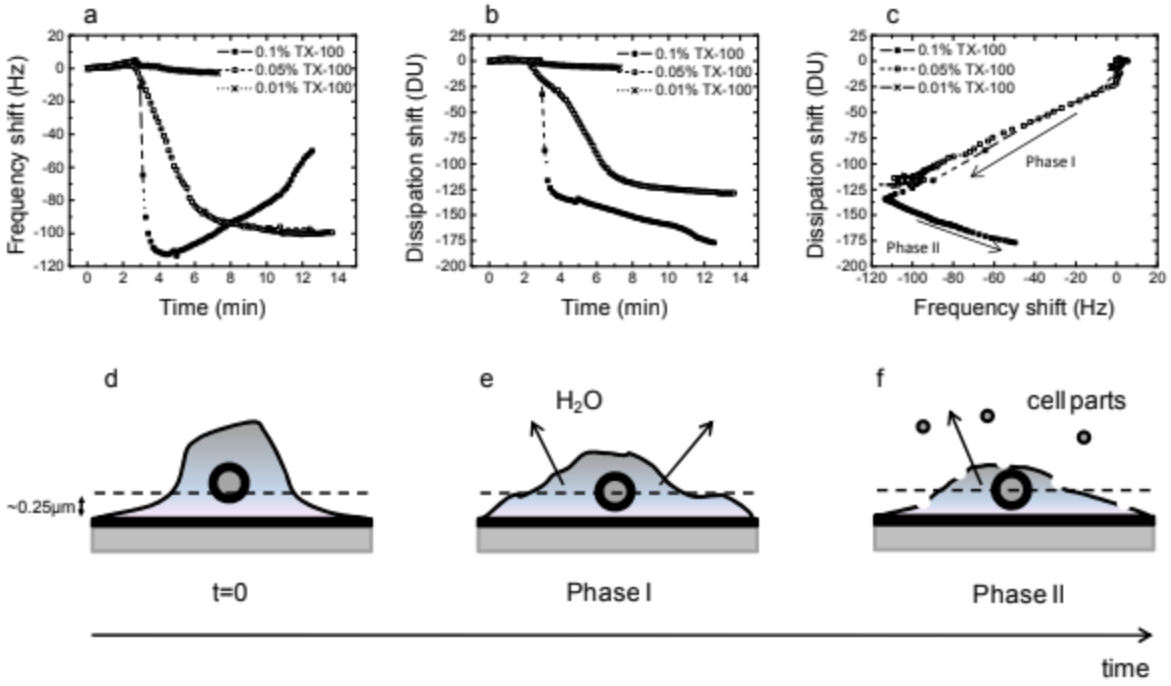

We used direct microscopy to observe any cellular changes and to confirm our hypotheses based on the QCM-D signals described above. Figure S1 presents fluorescence microscopy (a to c) and SEM images (d and e) of BAEC obtained without (a and d) or after (b, c and e) contact of the cells with TX-100-supplemented medium. Due to the limitations of direct fluorescence imaging, the lytic effects of TX-100 are only observable by microscopy after a long time exposure and at high TX-100 concentrations. For high TX-100 concentration (0.1%), it was possible to observe cell lysis (as shown by the arrows in Figure S1c). Control experiments did not reveal any fluorescence bleaching under the conditions used (data not shown). Hence, the results observed during Phase II, after 4 minutes of 0.1% TX-100 injection (Figure 1), may be attributed to the cell lysis. Figure S1e reveals the "vestiges" of adhered cells that have adhered

and been lysed by TX-100, in comparison to an intact, non-treated cell (Figure S1d), thereby confirming the occurrence of cell lysis upon exposure to TX-100 under these conditions. Questions arise now regarding the effect of TX-100 during Phase I.

The observed decrease in both Δf and ΔD signals (Phase I) may be associated to a number of different phenomena. The QCM-D penetration signal is approximately 0.25 μm in water (Nimeri et al. 1998), allowing the detection of only a small portion of the adhered BAEC (~20 μm). When studying cell attachment, proteins present in the serum suspension rapidly adsorb onto the substratum thereby creating a conditioning film for the cells to attach onto and spread (Baier and Dutton 1969; Jurk and Kehrel 2005; Michelson 2002). One possible phenomenon is that TX-100 degrades this protein layer but control experiments conducted under the same conditions without BAEC on the crystal surface did not show any loss of mass (Figure S2a), hence, confirming that TX-100 is not acting on the underlying protein layer but rather on the cells directly. Figure S2a also shows the absence of signal shifts (Δf and ΔD are nearly the same with time) for experiments conducted with BAEC in non-supplemented medium. In order to accurately interpret the changes in Δf and ΔD observed in Figure 1 upon injection of TX-100, it is necessary to know how TX-100 can affect cells. TX-100 can solubilize the lipid bilayer and most integral membrane proteins that constitute the plasma membrane (Yu et al. 1973). Recently, Potgieter et al. (2009) used SEM to show that TX-100 at 0.0005% can severely disrupt the cell membranes after 24 hours without lysing them. During plasma membrane disruption, some intracellular components are released. Cells also release intracellular components (i.e., water) when they are placed in contact with a hyperosmotic medium. The presence of TX-100 in the medium may at first appear as hyperosmotic to the cells. The schematic representations in Figure 1 were drawn to illustrate the likely cellular changes corresponding with the QCM-D

signals obtained and correspond to the direct microscopy observation. Under hyperosmotic conditions, water is released; cells shrink, and tend to collapse on themselves (Figure 1e). Cell shrinkage would appear as a greater and more rigid detectable mass because material denser than water will "fall" within the signal penetration volume. This will result in a decrease in frequency and dissipation, as observed in Figures 1a to 1c. Figures S1b, c and e show no evidence of cell shrinkage as the resolution of fluorescence microscopy with living cells does not permit the measurement of such cell behavior with accuracy. To confirm the occurrence of cell shrinkage during Phase I, another experiment was conducted using medium supplemented with 100 mM NaCl in order to increase the osmotic pressure in a controlled manner. The *Df* plot obtained for this experiment (inset in Figure S2b) was nearly identical as that obtained with 0.1% TX-100 (Phase I). Control tests revealed that TX-100 induced irreversible changes (Δf and ΔD continue to decrease even after post-treatment wash, Figure S2c) while NaCl induced reversible changes (Δf and ΔD returned back nearly to their baseline values after post-treatment wash, Figure S2b). These observations suggest that even though TX-100 may first appear as a hyperosmotic agent to the BAEC (Phase I, short process), it does not function in the same manner as the less toxic NaCl, since TX-100 lytic effect was observed during Phase II (Figure S1), which is a notably longer process. From these observations, it is reasonable to conclude that the *Df* plot obtained (Figure 1c) is the signature response during BAEC membrane disruption.

3.2. Real-time monitoring of cellular response to LPS exposure

Lipopolysaccharides (LPS) act as endotoxins and have been identified as a major pathogenic factor in Gram-negative septic shock (Frey and Finlay 1998; Morrison and Ryan 1987). LPS from *Escherichia coli* can induce injury and disease by a variety of pathways, many of which

could result in morphological changes of mammalian cells (Morrison and Ulevitch 1978). As opposed to TX-100, LPS will induce cell rounding (Chakravortty et al. 2000). In an effort to evaluate whether QCM-D can discriminate the effects of different cytomorphic agents (TX-100 vs. LPS), additional experiments were conducted using LPS-supplemented media.

Figure 2 shows that, in contrast to TX-100, exposure to LPS resulted in a single-phase QCM-D signal: Δf steadily increased (when Δf was decreasing in the case of TX-100) while ΔD decreased, meaning that less mass is detected in the sensing region. As with TX-100, control experiments conducted without cells did not show any significant change in Δf or ΔD following injection of LPS laden medium (Figure S2a), indicating that LPS does not act on the supporting protein layer. As LPS concentration increased from 25 to 250 μg/mL in the medium, the QCM-D responses for both Δf and ΔD were faster, as expected (Figures 2a and 2b, respectively). Since Δf and ΔD are equally affected by the change in concentration, the resulting Df plots all have the same slope, as indicated in Figure 2c (p=0.99). This is similar to what was observed for TX-100 experiments. As indicated previously, the shape of the Df plot may be an indication that mass is being removed from the quartz crystal sensor. The changes in Δf and ΔD can be explained by describing the actual effect of LPS on the BAEC cytoskeleton. Chakravortty et al. (2000) observed cell rounding for BAEC cultured in LPS-supplemented medium. LPS induced cellular retraction in endothelial cells was also noticed by Meyrick et al. (1989; 1986). As illustrated in the schematic diagrams of Figure 2 (d to f), the rounding of the cells would cause a progressive loss of detected mass and dissipation by the quartz sensor within the sensing volume (Figures 2e and 2f) as compared with a non-treated cell (Figure 2d). This phenomenon is theoretically represented by an increase in Δf and a decrease in ΔD, as observed in Figure 2 (a to c).

Figure 2. Representative QCM-D measurements (a) frequency and (b) dissipation shifts, (1st overtone) for BAEC response to different concentrations of LPS as a function of time and (c), *Df* plot resulting from (a) and (b) curves: 250 µg/mL LPS (▲ symbols and solid line), 100 µg/mL LPS (△ symbols and dashed line), 50 µg/mL LPS (▼ symbols and dotted line) and 25 µg/mL LPS (▽ symbols and dashed dotted line). (d), (e) and (f), schematic diagrams representing the effect of LPS on BAEC with time, starting with a non-treated cell (t=0, d).

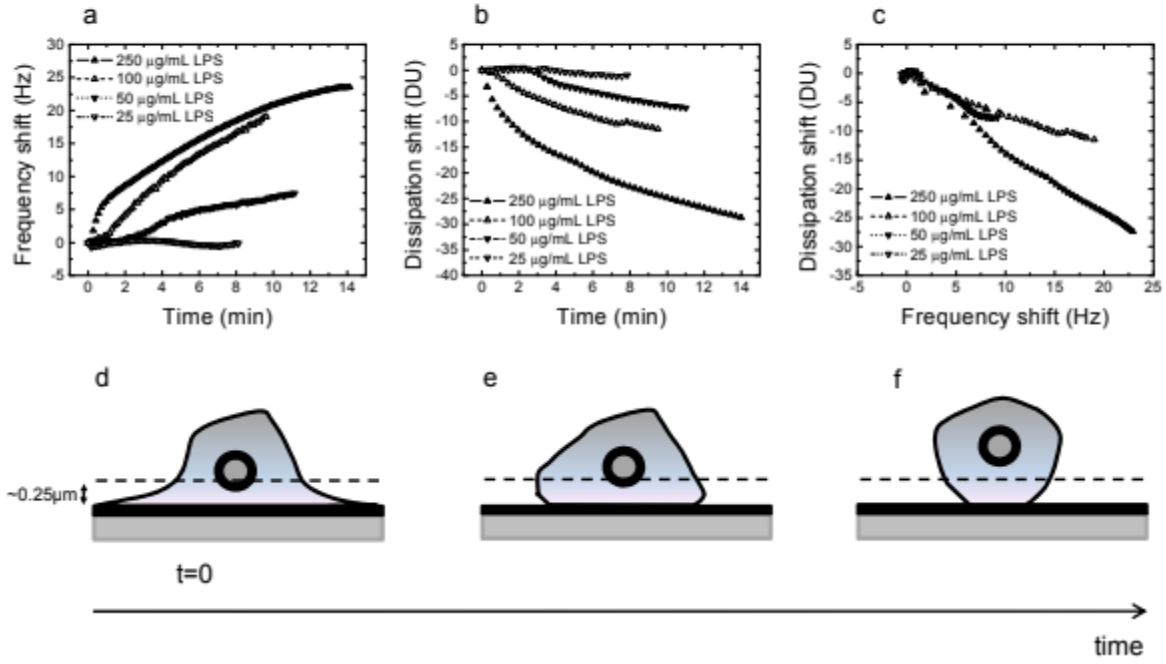

Fluorescence and electron microscopy (Figures S3a to S3c and S3d to e, respectively) showed cell rounding of BAEC for the highest concentration of LPS tested (250 µg/mL), thereby confirming the analysis of the QCM-D response described in Figure 2. It was also noted that, like the experiments conducted with TX-100, significant morphological changes were only observed by fluorescence microscopy when BAEC were exposed to LPS for long time periods (20-30 minutes) and at high concentrations due to the limitations of live cell imaging techniques, while the QCM-D was able to detect changes within the first few minutes of exposure to LPS and even at low concentrations.

3.3. Effect of cell toxins and reagents on cell morphology: Comparison of Df plots obtained from BAEC responses to cytomorphic agents

As complementary analysis, we completed linear regression analyses of initial Δf and ΔD slopes as a function of LPS concentration. This analysis resulted in linear correlation coefficients of 0.98 and 0.88 for Δf and ΔD slopes, respectively, while during Phase I of TX-100 experiments, initial Δf and ΔD changes with time were exponentially correlated with TX-100 concentration (data not shown). These results suggest that the TX-100 effect could predominate over the LPS effect when these two cytomorphic agents are mixed together in high concentrations. To actually examine whether the QCM-D technique could be used to evaluate if different cytotoxin effects can act in competition through real-time QCM-D monitoring, additional experiments were carried out using media supplemented with combinations of LPS and TX-100. Table S1 shows the *Df* slopes obtained for these experiments. For 0.01% TX-100 + 100 µg/mL LPS, the *Df* slope obtained (~ -0.74 DU/Hz) is in the range of that obtained for the LPS series average. This means that the action of LPS predominates over TX-100 under these conditions. For the experiment conducted with 100 µg/mL LPS and 0.1% TX-100, the QCM-D response (*Df* slope=0.63 DU/Hz) was closer to that obtained for the TX-100 alone (~0.89 DU/Hz, averaged value for TX-100 series), implying that at this higher concentration, the effect of TX-100 induces a "faster" QCM-D response than 100 µg/mL LPS, as already suggested by the regression analyses. In the third "mixture" experiment, (0.025% TX-100 + 100 µg/mL LPS), the *Df* plot (Figure 3) tends at first to follow the *Df* plot obtained for 100 µg/mL LPS alone but the *Df* slope obtained along the linear portion of the signal is different (*Df* slope=-0.47 DU/Hz compared to -0.74 DU/Hz for the LPS series), thus indicating that another action other than LPS' is taking

place simultaneously. It is interesting to note that by the end of the curve, the *Df* slope actually approaches that obtained for the TX-100 series, providing it with a different signature.

Figure 3. Representative *Df* plots for BAEC response to medium supplemented with 100 µg/mL HFN (○ symbols and short dotted line), 100 µg/mL LPS (△ symbols and dashed line), 0.1% TX-100 (■ symbols and solid line), 100 µg/mL LPS and 0.025% TX-100 (⬟ and dashed dotted line). The control experiment with BAEC alone (without cytomorphic agent) is not displayed in this plot since it would be represented by just a few points around the *f*=0 and *D*=0 origin.

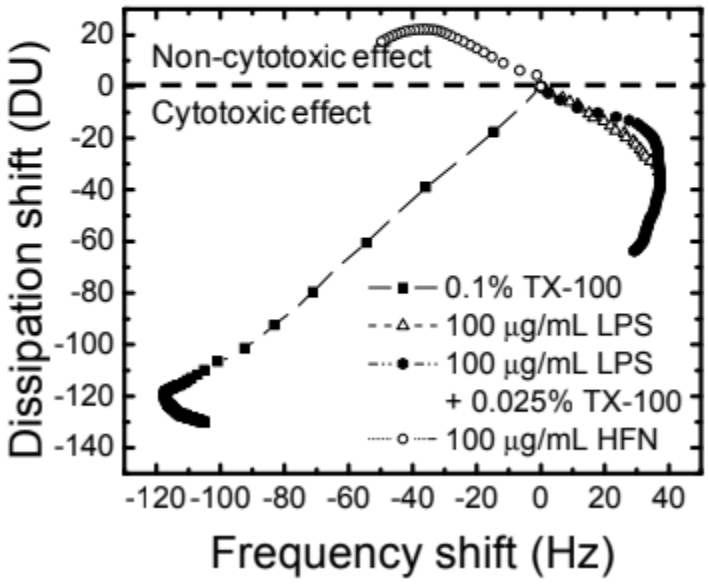

Figure 3 also highlights the difference in the BAEC signature responses between LPS and TX-100. Our results suggest that different mechanical or biochemical pathways can result in different *Df* plots using QCM-D. To confirm that QCM-D can distinguish between a cytotoxic and non-cytotoxic response, experiments were also carried out with non-cytotoxic agents promoting cell growth (addition of 10 mg/mL HFN to the medium or using a higher serum concentration (20%)). Figure 3 presents the *Df* plot obtained for medium supplemented with HFN. A similar *Df* plot was obtained when a supplementary amount of serum was added to the growth medium (data not shown). The *Df* plot obtained for the non-cytotoxic agents (HFN or additional serum) tends in a direction opposite to the plots obtained for the cytotoxic agents (TX-

100 and LPS); namely, frequency decreased while dissipation increased (all data points fall above the dashed line in Figure 3). This result may be attributed to serum proteins adsorbing at the cells' surface. Fibronectin is also known to be a thrombogenic protein promoting cell adhesion and spreading (Michelson 2002; Woods et al. 1986). In the latter part of the experiment, cells started to slowly spread on the substratum surface. Their anchorage point at the sensor surface became stronger as specific serum proteins adsorbed, thus providing more rigidity to the interaction between the sensor surface and the BAEC. This phenomenon resulted in a slow and small decrease in the Df factor; Δf was nearly not affected (Figure 3). Fatisson et al. (2008) measured a decrease in the Df factor when pseudopodia appeared following adherence of blood platelets onto thrombogenic surfaces. The spreading effect of HFN on BAEC could not be observed by fluorescence microscopy or SEM (data not shown) under the conditions tested due to the limitations of such techniques as previously pointed out. Hence, QCM-D appears again as a more sensitive technique to detect such small changes in living cells in comparison with microscopy techniques.

4. Conclusions

Cytoskeletal changes in living cells can be reproducibly monitored by QCM-D. Results show that the cell response to different cytomorphic agents can generate different QCM-D signals. These signatures are characteristic of cell morphology changes (cell shrinkage and lysis due to TX-100 effect, cell rounding induced by LPS), resulting from different mechanical and/or biochemical pathways. This study also indicates that cell toxicity can be predicted since cytotoxic agents induce a decrease in dissipation, while non-cytotoxic agents lead to a normal increase in dissipation. Furthermore, cell response to chemical stressors could be detected in a

unique manner with live cells, in real-time, at early stages and at relatively low concentrations of chemicals. This technique has potential use in cytotoxicity assays (differentiation of necrosis vs apoptosis) as well as in drug testing on cells with a clarified response in real-time, at lower drug concentrations than those used by other techniques.

Acknowledgements

This work was supported by l'Institut (Robert Sauvé) de Recherche sur la Santé et la Sécurité au Travail, the Natural Sciences and Engineering Research Council of Canada, the Fonds Quebecois de la Recherche sur la Nature et les Technologies, and the Canada Research Chairs program. We acknowledge Che O'May, Cathy Tkaczyk and Richard Leask (McGill University) for helpful discussions, Hojatollah Vali (McGill University) for providing access to his laboratory for cell culture and Lyne Nadeau (McGill University) for help in the statistical analysis.

References

Alessandrini, A., Croce, M.A., Tiozzo, R., Facci, P., 2006. Appl. Phys. Lett. 88(8), 083905/083901-083905/083903.
Baier, R.E., Dutton, R.C., 1969. J. Biomed. Mater. Res. 3(1), 191-206.
Basu, I., Mitra, R., Saha, P.K., Ghosh, A.N., Bhattacharya, J., Chakrabarti, M.K., Takeda, Y., Nair, G.B., 1999. FEMS Microbiol. Lett. 179(2), 255-263.
Chakravortty, D., Koide, N., Kato, Y., Sugiyama, T., Kawai, M., Fukada, M., Yoshida, T., Yokochi, T., 2000. Clinical and Diagnostic Laboratory Immunology 7(2), 218-225.
Cooper, M.A., Singleton, V.T., 2007. J. Mol. Recognit. 20(3), 154-184.
Elsom, J., Lethem, M.I., Rees, G.D., Hunter, A.C., 2008. Biosens. Bioelectron. 23(8), 1259-1265.
Fatisson, J., Merhi, Y., Tabrizian, M., 2008. Langmuir 24(7), 3294-3299.
Fredriksson, C., Khilman, S., Kasemo, B., Steel, D.M., 1998a. J. Mater. Sci.: Mater. Med. 9(12), 785-788.
Fredriksson, C., Kihlman, S., Rodahl, M., Kasemo, B., 1998b. Langmuir 14(2), 248-251.
Frey, E.A., Finlay, B.B., 1998. Microb. Pathog. 24(2), 101-109.
Goldblum, S.E., Ding, X., Brann, T.W., Campbell-Washington, J., 1993. J. Cell. Physiol. 157(1), 13-23.
Hosoya, N., Mitsui, M., Yazama, F., Ishihara, H., Ozaki, H., Karaki, H., Hartshorne, D.J., Mohri, H., 1993. J. Cell Sci. 105(4), 883-890.
Ives, C.L., Eskin, S.G., McIntire, L.V., 1986. In vitro cellular & developmental biology: journal of the Tissue Culture Association 22(9), 500-507.
Jurk, K., Kehrel, B.E., 2005. Semin. Thromb. Hemost. 31(4), 381-392.
Kabir-Salmani, M., Shiokawa, S., Akimoto, Y., Hasan-Nejad, H., Sakai, K., Nagamatsu, S., Sakai, K., Nakamura, Y., Hosseini, A., Iwashita, M., 2002. J. Clin. Endocrinol. Metab. 87(12), 5751-5759.
Kanazawa, K.K., Gordon, J.G., II, 1985. Anal. Chim. Acta 175, 99-105.
Lord, M.S., Modin, C., Foss, M., Duch, M., Simmons, A., Pedersen, F.S., Milthorpe, B.K., Besenbacher, F., 2006. Biomaterials 27(26), 4529-4537.
Lord, M.S., Yu, W., Cheng, B., Simmons, A., Poole-Warren, L., Whitelock, J.M., 2009. Biomaterials 30(28), 4898-4906.
Marx, K.A., Zhou, T., Montrone, A., McIntosh, D., Braunhut, S.J., 2007. Anal. Biochem. 361(1), 77-92.
Marx, K.A., Zhou, T., Montrone, A., Schulze, H., Braunhut, S.J., 2001. Biosens. Bioelectron. 16(9-12), 773-782.
Marx, K.A., Zhou, T., Warren, M., Braunhut, S.J., 2003. Biotechnol. Prog. 19(3), 987-999.
Meyrick, B., Hoover, R., Jones, M.R., Berry, L.C., Jr., Brigham, K.L., 1989. J. Cell. Physiol. 138(1), 165-174.
Meyrick, B.O., Ryan, U.S., Brigham, K.L., 1986. Am. J. Pathol. 122(1), 140-151.
Michelson, A.D., 2002. Platelets.
Modin, C., Stranne, A.L., Foss, M., Duch, M., Justesen, J., Chevallier, J., Andersen, L.K., Hemmersam, A.G., Pedersen, F.S., Besenbacher, F., 2006. Biomaterials 27(8), 1346-1354.
Morrison, D.C., Ryan, J.L., 1987. Annu. Rev. Med. 38, 417-432.
Morrison, D.C., Ulevitch, R.J., 1978. Am. J. Pathol. 93(2), 526-618.
Nimeri, G., Fredriksson, C., Elwing, H., Liu, L., Rodahl, M., Kasemo, B., 1998. Colloids Surf. B 11(5), 255-264.
Okahata, Y., Kimura, K., Ariga, K., 1989. J. Am. Chem. Soc. 111(26), 9190-9194.
Potgieter, M., Pretorius, E., Oberholzer Hester, M., 2009. Ultrastruct. Pathol. 33(3), 93-101.
Redepenning, J., Schlesinger, T.K., Mechalke, E.J., Puleo, D.A., Bizios, R., 1993. Anal. Chem. 65(23), 3378-3381.
Rodahl, M., Hoeoek, F., Kasemo, B., 1996. Anal. Chem. 68(13), 2219-2227.
Rodahl, M., Hook, F., Fredriksson, C., Keller, C.A., Krozer, A., Brzezinski, P., Voinova, M., Kasemo, B., 1997. Faraday Discuss. 107(Interactions of Acoustic Waves with Thin Films and Interfaces), 229-246.
Rosenthal, K.S., Koussaie, F., 1983. Anal. Chem. 55(7), 1115-1117.
Rotsch, C., Radmacher, M., 2000. Biophys. J. 78(1), 520-535.
Sauerbrey, G., 1959. Zeitschrift fuer Physik 155, 206-222.
Tufenkji, N., Rifai, O.J., Harmidy, K., Eydelnant, I.A., 2010. Food Res. Int. 43(3), 922-924.
Walter, I., Egerbacher, M., Wolfesberger, B., Seiberl, G., 1998. Scanning 20(7), 511-515.
Woods, A., Couchman, J.R., Johansson, S., Hook, M., 1986. Embo. J. 5(4), 665-670.
Yamaguchi, K., Nomura, S., Kido, H., Kawakatsu, T., Fukuroi, T., Suzuki, M., Hamamoto, K., Yanabu, M., Kokawa, T., Yasunaga, K., 1993. Am. J. Hematol. 44(2), 106-111.
Yu, J., Fischman, D.A., Steck, T.L., 1973. J. Supramol. Struct. 1(3), 233-248.
Zhou, T., Marx, K.A., Warren, M., Schulze, H., Braunhut, S.J., 2000. Biotechnol. Prog. 16(2), 268-277.